Preparation of Nanoparticles Composed of Chitosan and Its Derivatives as Delivery Systems for Macromolecules

Yan Sun, Ajun Wan

Department of Chemistry, School of Chemistry and Chemical Technology, Shanghai Jiao Tong University, 200240 Shanghai, People's Republic of China

Received 25 April 2006; accepted 16 December 2006
DOI 10.1002/app.26038
Published online 27 March 2007 in Wiley InterScience (www.interscience.wiley.com).

ABSTRACT: Three different kinds of nanoparticles for paracellular transport were prepared using a simple and mild ionic-gelation method. Sodium tripolyphosphate (TPP) as crosslinking agent was added into three kinds of solutions, which were chitosan solution, physical blending solution of chitosan, and glycidyl trimethylammonium chloride (GTMAC), and *O*-(2-hydroxyl) propyl-3-trimethyl ammonium chitosan chloride (O-HTCC) solution respectively. O-HTCC was synthesized by coupling of GTMAC to chitosan whose functional groups of the NH_2 groups were protected. The nanoparticles were characterized by transmission electron microscopy, atomic force microscopy, photon correlation spectroscopy, and zeta potential measurement. The results showed that increasing TPP concentration promoted the size of chitosan nanoparticles, a decrease in the size of O-HTCC nanoparticles incurred on the contrary. The size of O-HTCC nanoparticles is slightly bigger than that of pure chitosan nanoparticles, and smaller than that of physical blending nanoparticles (PBN). Bovine serum albumin (BSA), as a model protein drug, was incorporated into the nanoparticles. Compared with chitosan nanoparticles and PBN, high BSA loading efficiency (87.5%) and loading capacity (99.5%) are achieved by quaternized chitosan (O-HTCC) nanoparticles, and the release profile of BSA from nanoparticles has an obvious burst effect and a slowly continuous release phase followed. © 2007 Wiley Periodicals, Inc. J Appl Polym Sci 105: 552–561, 2007

Key words: chitosan; O-HTCC; nanoparticles; drug release; macromolecules

INTRODUCTION

Today, drug delivery seems to be the topic of interest with a better understanding of the basics in chitin and chitosan chemistry, mainly chemical modifications, biodegradation, effects on various tissues, distribution to various body organs, mucoadhesion, association of chitosan with inorganic compounds, and advanced technological transformations. The key considerations that justify this interest are that chitosan is biocompatible and does not elicit adverse reactions when in contact with human cells. Chitosan can be degraded by ubiquitous enzymes in the human body, and oligomers can activate macrophages and stimulate synthesis of hyaluronan. Moreover, they provide building blocks for the reconstruction of extracellular matrix components. On the other hand, chitosan is recognized by tumor cells, and therefore, it can bring drugs to their targets selectively. Chitosan is a safe and friendly substance for the human organism; therefore, medical and pharmaceutical applications can easily be worked out with joint efforts from specialists in various fields. However, these activities are limited to acidic conditions because of its poor solubility above pH $\sim$ 6.5, where chitosan starts to lose its cationic nature.[1–4] Chitosan is generally insoluble under physiological conditions because of a strongly hydrogen-bonding network structure. Thus, further investigations for the biological activities and development have been restricted. Water solubility is important in applications of chitosan as a pharmacologically active agent, and researchers have focused on the preparation of chitosan derivatives soluble in water over a wide pH range. Various water soluble compounds were synthesized by chemical modification.[5,6] The N-carboxymethylated, N,O-sulfated, and N-trimethylated chitosan derivatives showed reasonable low electric resistance.[7] Recently, Minoru Morimoto have synthesized carbohydrate-branched chitosan derivatives to get water solubility and novel biological activates.[8,9] A carbohydrate is one constituent of organisms and is a key molecule in an intercellular recognition and adhesion.[10] Highly cationic chitosan was prepared. Curti et al.[11] reported an alternative method exploring functionalized compounds such as choline dichloride carrying the preformed trimethylammonium

Correspondence to: A. J. Wan (wanajun@sjtu.edu.cn).
Contract grant sponsor: National Natural Science Foundation of China; contract grant numbers: 20376045, 20676079.
Contract grant sponsor: Nanometer Technology Program of Science and Technology Committee of Shanghai; contract grant number: 0452nm037.

Journal of Applied Polymer Science, Vol. 105, 552–561 (2007)

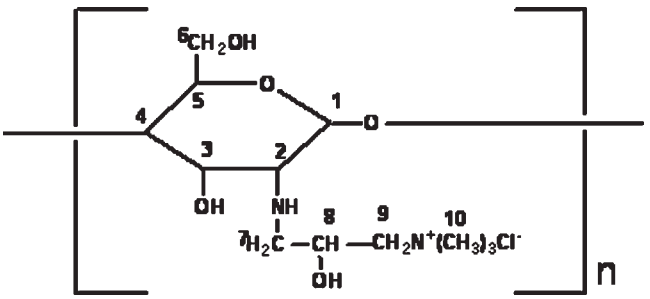

Figure 1 HTCC structure.

group that can react with chitosan to yield highly cationic chitosan. *N*-[(2-Hydroxy-3-trimethyl-ammonium)-propyl] chitosan chloride (HTCC) was prepared by reacting chitosan with glycidyl trimethylammonium chloride (GTMAC). HTCC structure is shown in Figure 1.[12]

Polymeric quaternary ammonium compounds have received the most attention as biocidal polymers over the years.[6] Now, major concerns with the antimicrobial agents used for human are their safety toward the human body. The antimicrobial activity of chitosan against a variety of bacteria and fungi coming from its polycationic nature, is well known.[12]

Biodegradable polymeric nanoparticles made from natural or synthetic polymers have drawn significant attention because of higher stability, maneuverability for industrial manufacture, and opportunity for further surface engineering.[13] They can be tailor-made to achieve both controlled drug release and site-specificity by tuning the polymer characteristics and surface chemistry.[14–16] It has been established that nanocarriers can get concentrated preferentially in certain disease sites, such as solid tumor, by virtue of the enhanced permeation and retention mechanism.[17] Once accumulated at the tumor site, they can act as a local drug depot depending upon the makeup of the carrier, thus providing a source for a continuous supply of encapsulated therapeutic compound into the tumor mass.[18–21] To prolong the systemic circulation time of the nanoparticles and hence enhance their passive targeting efficiency, various strategies that involve increasing positive charge on the surface of nanoparticles and creation of a hydrophilic sheath around the nanoparticles have been employed.[22,23] Quaternized chitosan has potential to be used as an absorption enhancer across intestinal epithelial cells due to its cationic nature, mucoadhesive, and permeability enhancing property.[24]

On the basis of this previous information, the major goal of the work presented here is to prepare O-HTCC, which was synthesized by coupling of GTMAC to chitosan, whose functional groups of the NH_2 groups were protected, and create new nanoparticles appropriately modified and to evaluate their potential as protein carriers. O-HTCC nanoparticles, chitosan nanoparticles and physical blending nanoparticle (PBN) were prepared. Those quaternaminated by GTMAC display the highest adsorption of endothelial cells due to quaternary aminonium group of strongly electro-static attraction with the negatively charged endothelial cells.[25] The structure of O-HTCC is given below (Fig. 2).

The physicochemical properties of these nanoparticles were analyzed by FTIR, photon correlation spectroscopy (PCS), zeta potential analysis, atomic force microscopy (AFM), and transmission electron microscopy (TEM). Bovine serum albumin (BSA) was designated as the model protein. BSA-loaded nanoparticles were prepared without any organic solvents and high-energy sources and characterized for their loading efficiency and loading capacity and *in vitro* release behavior.

EXPERIMENTAL

Materials

Chitosan from a shrimp shell was purchased from (Jinhu Co., China), deacetylation degree was 92%, and molecular weight (Mw) was 670 kDa (M67). BSA with Mw 68 kDa (M68) were purchased from Sigma Chemical Co. (USA). GTMAC was obtained from Dongying Guofeng Fine Chemical Co. (Shandong, China). All other chemicals were of reagent grade.

Preparation of O-HTCC

Conjugation of *N*-benzylidene chitosan

Chitosan was modified by the chemical conjugation of benzoyl hydride in the presence of solvent, alcohol. Chitosan (3.0 g) was dissolved in 10% acetic acid solution (100 mL). After the addition of benzoyl hydride (15.8 g), the solution was stirred for another hour, then placed for 20 h in vacuum (55–60°C). The polymer was adjusted to 7.0 with 1*N* NaOH solutions. The resulting solution was filtered and precipitate was washed with methanol several times.

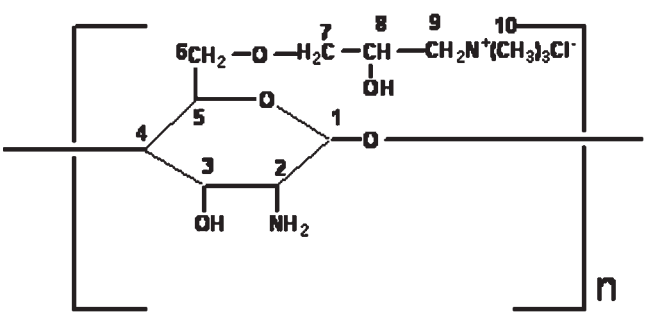

Figure 2 Structure of O-HTCC.

Synthesis of *O*-quaternary aminonium-*N*-benzylidene chitosan

Isopropyl alcohol (50 mL) and glycidyl-trimethyl-ammonium chloride (GTMAC) (9.0 g) were added to the *N*-benzylidene chitosan (9.0 g). The resulting mixture was stirred at 70°C for 16 h. The precipitate was washed with methanol and acetone in turn.

O-HTCC preparation

The volume of 50 mL of 0.25 mol/L HCl alcohol solution was added to *O*-quaternary aminonium-*N*-benzylidene chitosan (3.0 g), and then under stirring for 24 h at room temperature. After most of the alcohol was removed, 15 mL H_2O was added to the mixture, which was deposited by acetone. After being dried in vacuum (80°C), the O-HTCC was obtained.

Further purification of O-HTCC

O-HTCC (1.5 g) was dissolved in distilled water (40 mL), and then the solution was poured into adequate acetone to obtain the precipitate, which was filtered and washed with acetone several times. The obtained precipitate was dissolved in some distilled water once more, and dialyzed against distilled water for 3 days, concentrated, precipitated in acetone, and dried under vacuum at 80°C for 48 h to obtain the final pure product.

Preparation of chitosan nanoparticles, O-HTCC nanoparticles, and PBN

The content of the quaternary ammonium salt groups in the mixture was the same as that in O-HTCC. The accurate value of mixture was found for chitosan: GTMAC mole ratios 3.0 : 1.0. Chitosan, O-HTCC, and the mixture of chitosan and GTMAC were dissolved in acetic acid respectively. The concentration of three solutions was 1.0 mg/mL. Then, under stirring at room temperature, 0.8 mL sodium tripolyphosphate (TPP) aqueous solution with various concentrations (0.5, 1.0, 2.0, 2.5, 3.0, 4.0, 5.0 mg/mL) was added to 10 mL chitosan, O-HTCC and blending of chitosan and GTMAC solution respectively. Then samples were visually analyzed and three different systems were identified: solution, opalescent suspension, and aggregates. As tested in corresponding experiments, the zone of the opalescent suspension should be a suspension of nanoparticles we hope to acquire. It was found that when the concentration of TPP was in the range of 1.0–4.0 mg/mL, different sizes of nanoparticles could be obtained. When the concentration of TPP was below 1 mg/mL, solution was formed, and when the concentration of TPP was above 4 mg/mL, the aggregates were obtained.

Preparation of BSA-loaded nanoparticles

BSA-loaded nanoparticles were formed upon incorporation of TPP (2 mg/mL) and chitosan, O-HTCC and blending of chitosan and GTMAC solutions (1.0 mg/mL) containing BSA (1.0 mg/mL). Chitosan, O-HTCC, and blending of chitosan and GTMAC were dissolved in 10 mL acetic aqueous solutions, respectively. Then, 10 mg BSA was dissolved in above three solutions in turn. Finally, 0.8 mL of TPP solution was added to 10 mL of the above three kinds of solution, opalescent suspension was formed spontaneously under magnetic stirring at room temperature. The opalescent suspension was kept under stirring for 2 h.

Determination of BSA loading capacity and loading efficiency of nanoparticles

Loading capacity and loading efficiency of the different formations were determined by ultra-centrifugation of samples at 20,000 × *g* and 15°C for 30 min, the amount of free BSA was determined in clear supernatant by UV spectrophotometry at 280 nm using supernatant of their corresponding nonloaded BSA nanoparticles as basic correction. The BSA loading capacity (LC) of nanoparticles and BSA loading efficiency (LE) were calculated by using eqs. (1) and (2), respectively:[26]

$$\mathrm{LC} = (A - B)/C \times 100 \quad (1)$$

$$\mathrm{LE} = (A - B)/A \times 100 \quad (2)$$

where A is the total amount of BSA in added solution, B is the total amount of BSA in supernatant after centrifugation, and C is the weight of the nanoparticles measured after freeze-drying.

BSA release from the nanoparticles *in vitro*

The *in vitro* BSA release profiles of chitosan nanoparticles, O-HTCC nanoparticles, and PBN were determined as follows: the BSA-loaded nanoparticles separated from 18 mL suspension were placed into test tubes with 6 mL of 0.2 mol/L phosphate saline cushion liquid (PBS), and incubated at 37°C under stirring. At appropriate intervals, samples were ultracentrifuged, and 3 mL of the supernatant was replaced by fresh medium. The amount of BSA released from the nanoparticles was evaluated by UV spectrophotometry.

Physicochemical characterization of chitosan nanoparticles, O-HTCC nanoparticles, and PBN

The size and morphological measurements of the nanoparticles were performed by TEM-100CXII and AFM (Nanoscope E, Digital Instrument). The average particle size and size distribution were determined by PCS with a Malvern Zetasizer Nano S (Malvern Instruments Limited, United Kingdom). Zeta potential measurements of nanoparticles were performed by microelectrophoresis apparatus (Model BDL-B, Shanghai, China). IR spectra of chitosan, O-HTCC and O-HTCC nanoparticles, were taken with KBr pellets on Perkin–Elmer spectrum on FTIR.

RESULTS AND DISCUSSION

Physicochemical characterization of O-HTCC nanoparticles

FTIR study

In this experiment, O-HTCC was dialyzed against distilled water for 3 days. GTMAC that did not react with chitosan would be removed out from the system, and then there would be no special absorption band of GTMAC in the IR spectra of O-HTCC. In Figure 3, the IR spectra of native chitosan and the O-HTCC are shown. The absorption band at 1656 cm^{-1} in native chitosan was referenced as amide I bands, and the absorption band at 1606 cm^{-1} was ascribed to the N—H bending mode in the primary amine. The absorption band of $—NH_2$ in O-HTCC still existed, but shifted to the place at 1647 cm^{-1}, suggesting that N-alkylation in chitosan did not occur. Acetylamino I 1656 cm^{-1} overlapped with NH_2-associated band at 1647 cm^{-1}. Compared with chitosan, O-HTCC produced a band at 1487 cm^{-1}, which was attributed to the methyl groups of ammonium.[27] In addition, we can see that the absorption band at 1096 cm^{-1}, which was caused by $CH_2—O—CH_2$ of O-HTCC, was very obvious. This indicates that the reaction happened. The spectrum of O-HTCC nanoparticles is different from that of O-HTCC matrix. The intensity of 1487 cm^{-1} peak disappears and a new peak of 1545 cm^{-1} appears, which showed that TPP was linked with ammonium groups and $—N^+(CH_3)_3$ of O-HTCC in nanoparticles. Hydroxyl group absorption of chitosan at 1243 cm^{-1} almost disappears in O-HTCC nanoparticles, which indicates that free hydroxyl groups form hydrogen bonding.[25]

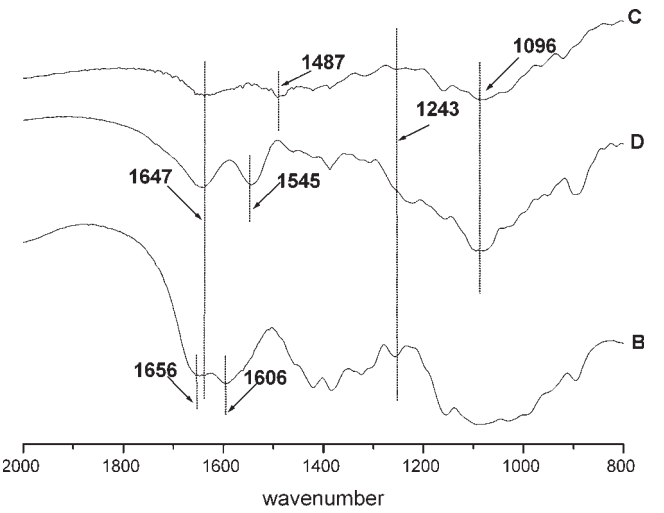

Figure 3 FTIR of (B) chitosan, (C) O-HTCC, and (D) O-HTCC nanoparticles.

^{1}H NMR analysis

Figure 4 shows the ^{1}H NMR spectra of the chitosan and the O-HTCC. The proton assignment of chitosan [Fig. 4(A)] is as follows: $\delta_{2.95}$ = CH (carbon 2 of chitosan); $\delta_{3.3–3.7}$ = CH (carbon 3–6 of chitosan); $\delta_{4.2–4.5}$

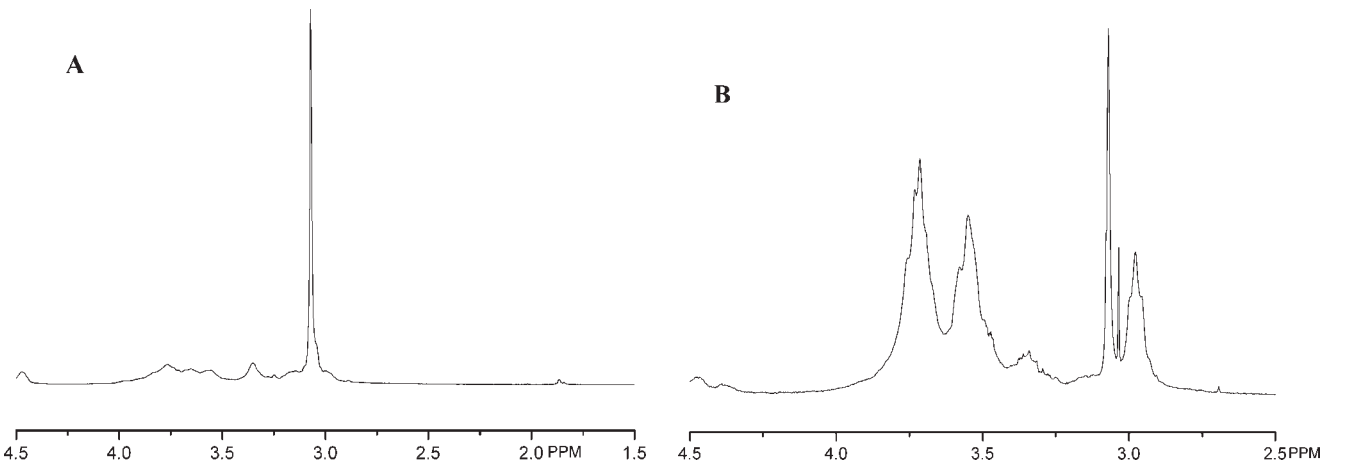

Figure 4 ^{1}H NMR spectra of (A) chitosan and (B) O-HTCC in CD_3COOD and D_2O.

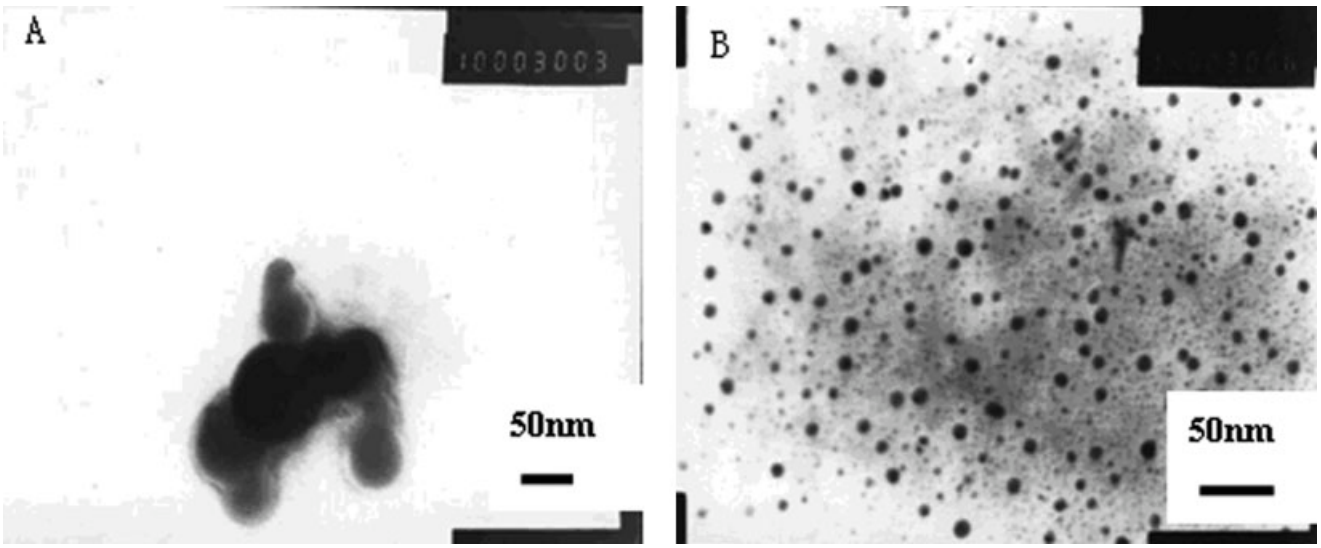

Figure 5 TEM of nanoparticles (A) pure chitosan (TPP 4 mg/mL) and (B) pure chitosan (TPP 1 mg/mL).

= CH (carbon 1 of chitosan).[26] The proton assignment of O-HTCC [Fig. 4(B)] is as follows: $\delta_{2.95}$ = CH (carbon 2 of chitosan). A new peak at 3.35 ppm, which originates from the ^{1}H NMR spectra of CH_2 (O—CH_2), is due to mainly characteristic methylene protons of the reacted chitosan hydroxyl group with quat ammonium salts.[28] This peak shows the presence of major functional groups linked to chitosan, and peak at 3.1 ppm is belong to three methyl protons of quat ammonium salt. The reaction happened between hydroxyl group on 6-C of chitosan and GTMAC. The degree of substitution (DS, %) value was determined from the relative ratio of the peak area of carbon 1 of O-HTCC at 4.2–4.5 ppm and the peak area of carbon 10 of O-HTCC at 3.1 ppm (methyl protons of trimethylammonium group), as seen in Figure 4. The DS increased gradually with reaction time and reached at the maximum value (33.3%) after 16 h, which indicates that the epoxide groups of GTMAC reacted with hydroxyl groups of the chitosan.

TEM analysis

At room temperature, an alkaline phase (pH = 7–9) containing TPP was added into an acidic phase (pH = 4–6) containing chitosan, then nanoparticles were formed immediately upon mixing of the two phases through inter and intra molecular linkages created between TPP phosphates and chitosan amino groups. Nanoparticles with varying characteristics can be obtained with different concentrations of chitosan and TPP, as well as by changing the relative

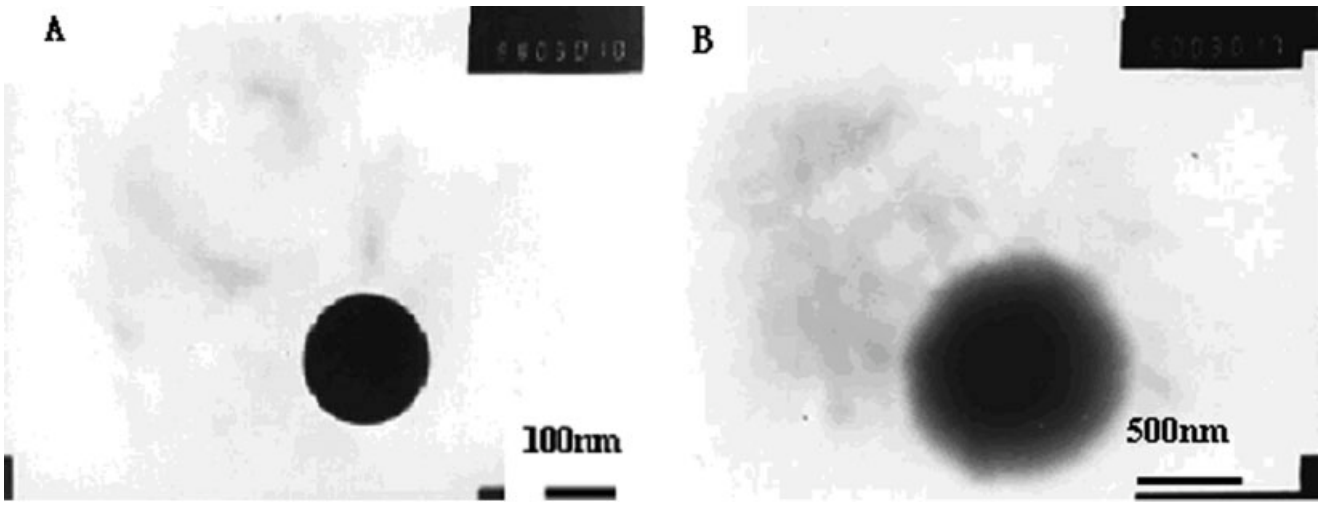

Figure 6 TEM of O-HTCC nanoparticles (A) TPP 4 mg/mL and (B) TPP 1 mg/mL.

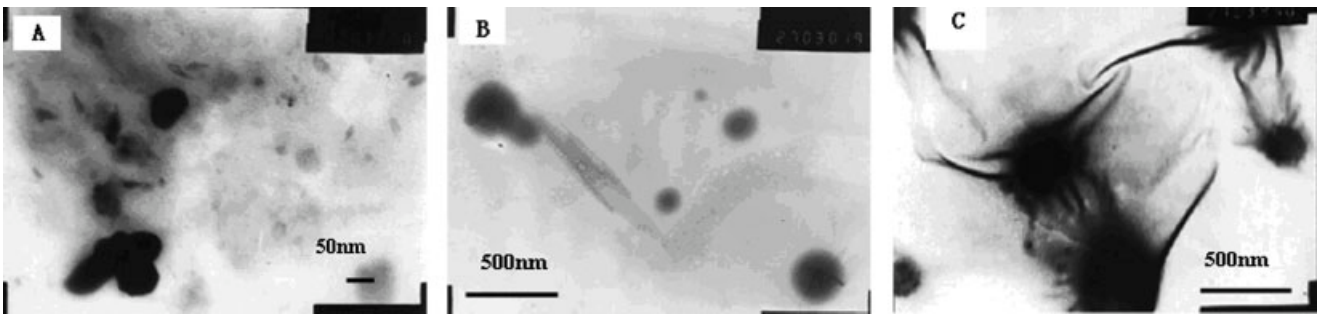

Figure 7 TEM of nanoparticles (A) chitosan, (B) O-HTCC, and (C) physical blending of chitosan and GTMAC: TPP 2 mg/mL.

volumes of the acidic and alkaline solutions. However, to produce a high yield of stable and solid nanometric structures, the chitosan: TPP weight ratio should normally be within the range 3 : 1 to 6 : 1.[29] The conditions for the formation of high yield nanoparticles with a particular nanometric size may vary significantly depending on the purity, acid salt, and molecular weight of chitosan employed. Consequently, the formulation parameters should be optimized for each individual chitosan type.[30,31]

The formation of nanoparticles is only possible for some specific concentration of chitosan and TPP, too high chitosan concentration (2.0 mg/mL) led to clear solution, no nanoparticles formation, and too high TPP concentration (5.0 mg/mL) led to aggregates with large size. As shown in Figure 5, the higher the initial concentration of TPP, the larger size of the chitosan nanoparticles, the size of nanoparticles is about 10 nm when the TPP concentration is 1 mg/mL, and when the TPP concentration is 4 mg/mL, the size of nanoparticles becomes larger to be about 100 nm. Figure 6 shows the size of O-HTCC nanoparticles increasing with decreasing TPP concentration, whose conclusion is different from that of the above chitosan (Fig. 5). At the same condition (TPP 2.0 mg/mL), chitosan nanoparticles are about 50–80 nm in size and more spherical and smoother compact morphological characteristic; chitosan nanoparticles modified by GTMAC are about 250 nm in size and more spherical and smoother but not compact morphological characteristic; nanoparticles are 500 nm in size and in irregular shape (Fig. 7), under conditions of physical blending of chitosan and GTMAC.

AFM analysis

The nanoparticles size, shape, and distribution could be observed from the AFM experiment. The self aggregates are spherical in shape and have a smooth surface (Figs. 8 and 9), whereas the mean diameter and size distribution are a little bit different from the TEM results. This might be due to the different conditions for sample preparation. For example, while the sample for TEM measurement was prepared by dispersing the particles in distilled water and then deposited on Formvar-coated 200–300 mesh copper grids and determined immediately in the hydrated

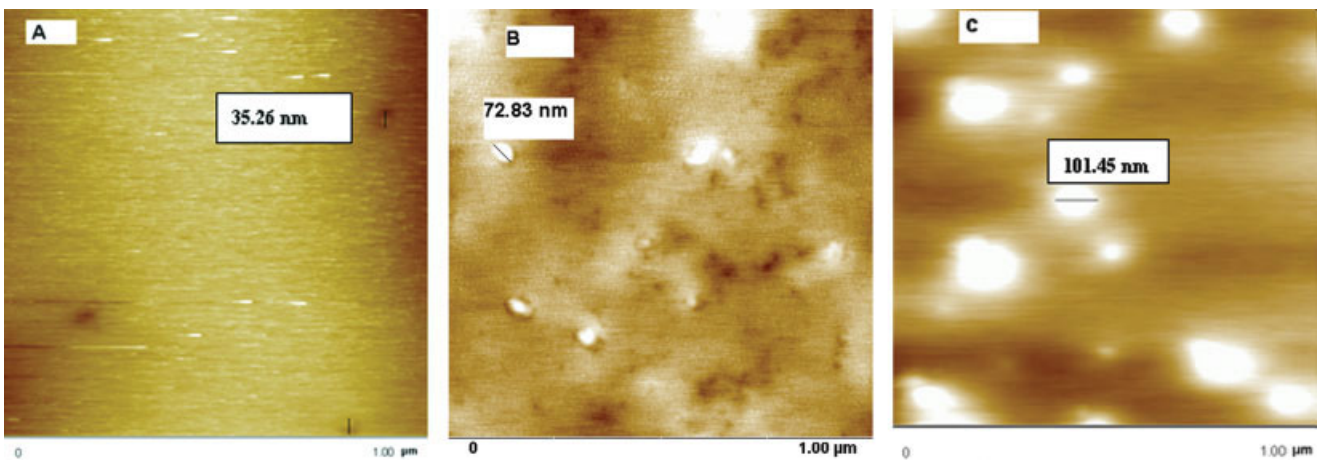

Figure 8 AFM image of O-HTCC nanoparticles: (A) TPP (4 mg/mL), (B) TPP (2.5 mg/mL), and (C) TPP (2.0 mg/mL). [Color figure can be viewed in the online issue, which is available at www.interscience.wiley.com.]

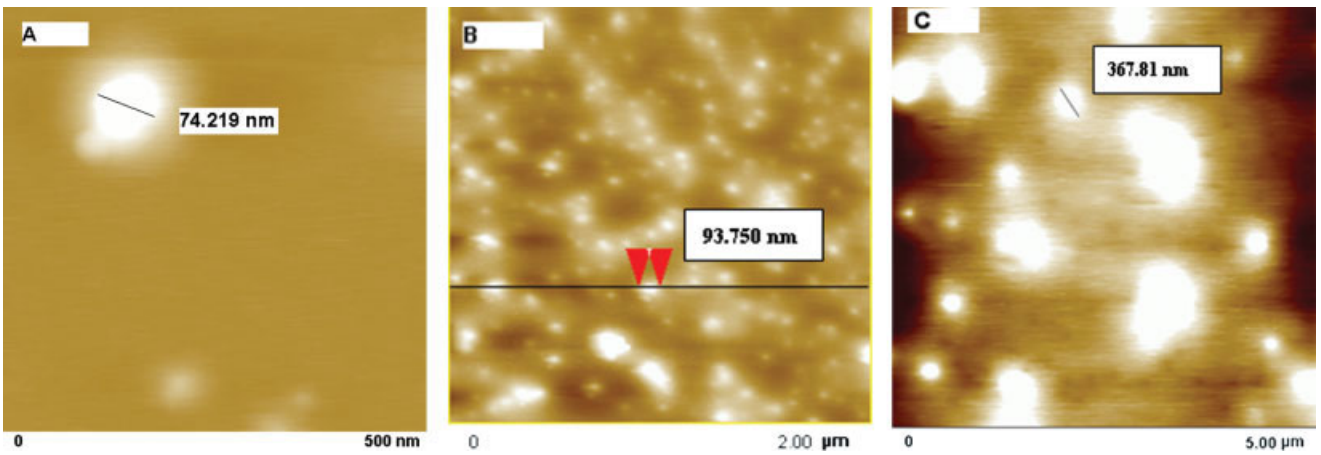

Figure 9 AFM image of nanoparticles of (A) pure chitosan, (B) O-HTCC, and (C) physical blending of chitosan and GTMAC: TPP 2.0 mg/mL. [Color figure can be viewed in the online issue, which is available at www.interscience.wiley.com.]

state, the sample for AFM was prepared in distilled water, and then deposited on sheet mica.[32]

Figure 8 shows the size of O-HTCC nanoparticles increasing with decreasing TPP concentration. At the same condition (TPP 2.0 mg/mL), the dimensions of chitosan nanoparticles, O-HTCC nanoparticles, and PBN were different, chitosan nanoparticles (about 75 nm) < O-HTCC nanoparticles (about 100 nm) < PBN (about 300–400 nm) (Fig. 9). The conclusion is the same as the result from the TEM. The size of O-HTCC nanoparticles is increasing with decreasing TPP concentration, which may be due to the compact structure. In TPP gelation process, there are three types of ionic interactions that contribute to the crosslinked networks of O-HTCC nanoparticles: electrostatic attraction between the electro-positive amino hydrogen of chitosan and the electro-negative anion of TPP, junction formed by tripolyphosphoric and $—N^+(CH_3)_3$ of O-HTCC and repel force between $—N^+(CH_3)_3$. Competition between three kinds of force exists during gelation process at the same time. When the TPP concentration is low, repel force between $—N^+(CH_3)_3$ is the strongest.[25] The structure of O-HTCC nanoparticles is looser, and the size of nanoparticles is larger than that of high TPP concentration.

PCS measurement

Figure 10 showed the results of nanoparticle size characterization by PCS, which is a dynamic light scattering method. In contrast to smaller and larger O-HTCC nanoparticles and PBN to be present at random demonstrated by TEM and AFM, PCS analysis, suggesting the unimodal size distributions, provides consistency above general law. PCS assigns average sizes of O-HTCC nanoparticles and PBN as ~ 265.4 and 516.6 nm, [Fig. 10(A,B)] respectively. Of course, the results from PCS are similar to that from TEM and AFM. However, the PCS value is a bit higher than that of TEM and AFM. One explanation for the differences can be ascribed to the underlying principles of their measurement methods. The contrast of TEM and AFM pictures allows only the visualization of the nanoparticles' core; conversely, PCS assesses the hydrodynamic radius of analytes.[33]

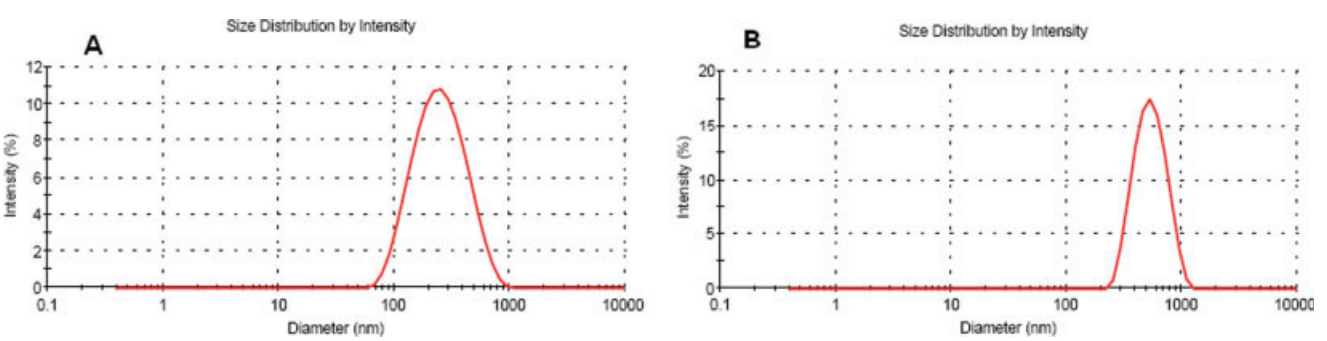

Figure 10 PCS analysis of nanoparticles of (A) O-HTCC and (B) physical blending of chitosan and GTMAC: TPP 2.0 mg/mL. [Color figure can be viewed in the online issue, which is available at www.interscience.wiley.com.]

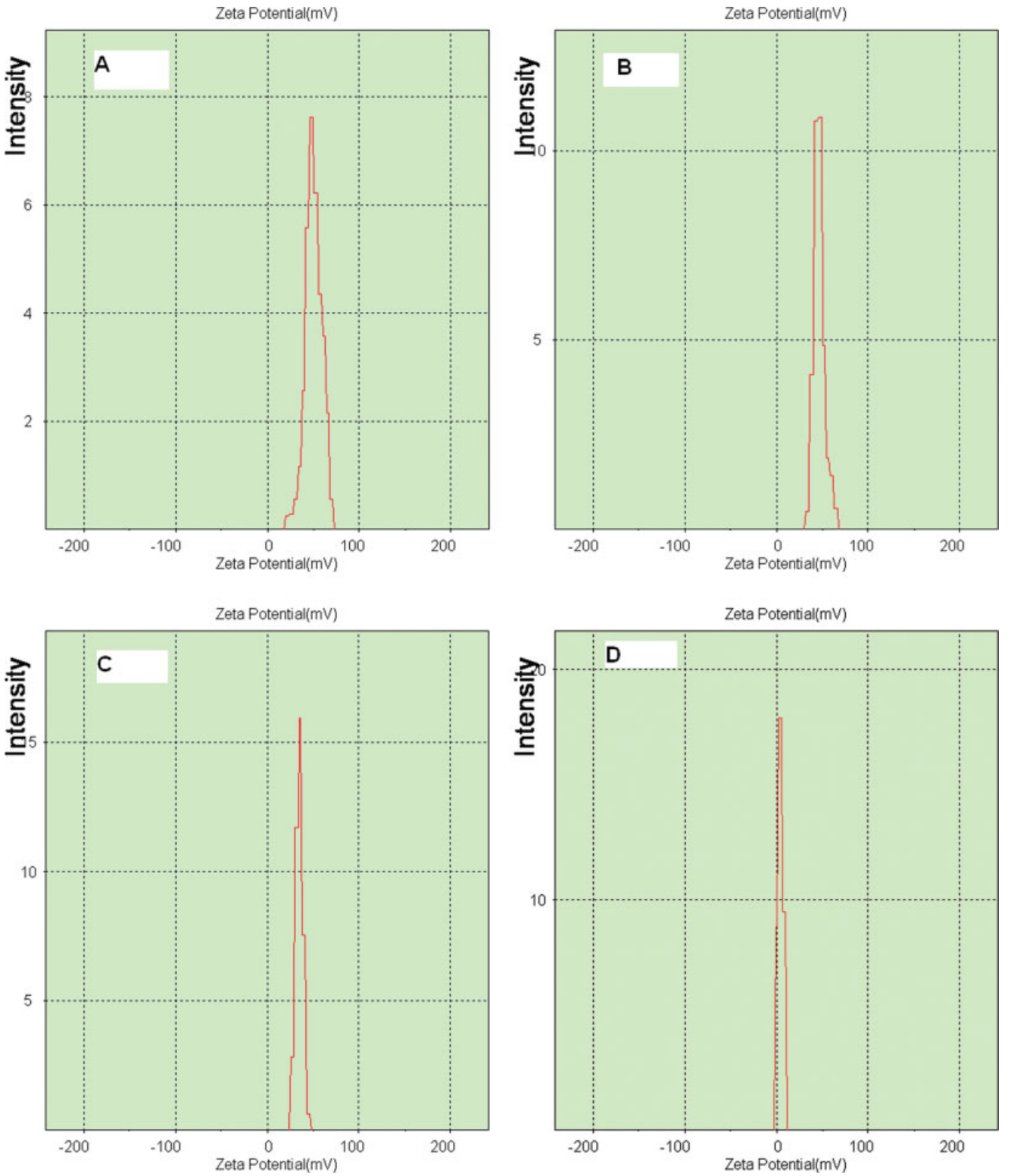

Figure 11 Zeta potential profiles of O-HTCC nanoparticles solution (A) ξ-potential 50.2 mV (TPP 1 mg/mL), (B) ξ-potential 47.8 mV (TPP 2 mg/mL), (C) ξ-potential 34.1 mV (TPP 3 mg/mL), and (D) ξ-potential 4.6 mV (TPP 4 mg/mL). [Color figure can be viewed in the online issue, which is available at www.interscience.wiley.com.]

Zeta potential measurement

Zeta potentials are often used as an important parameter in explaining the electrostatic surface interaction in adsorption.[34] Zeta potentials so determined from the fragments in the samples were used to represent the zeta potentials of the sample beads in solutions of the same pH values.[35]

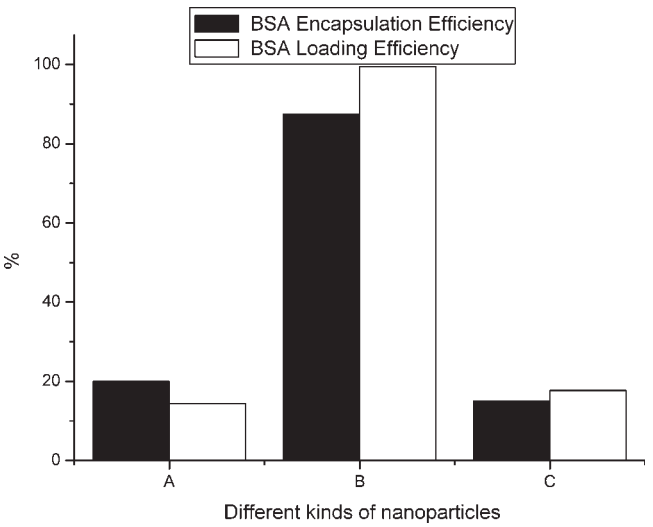

Figure 12 BSA loading capacity and efficiency of nanoparticles of (A) chitosan, (B) O-HTCC, and (C) physical blending of chitosan and GTMAC: TPP (2.0 mg/mL).

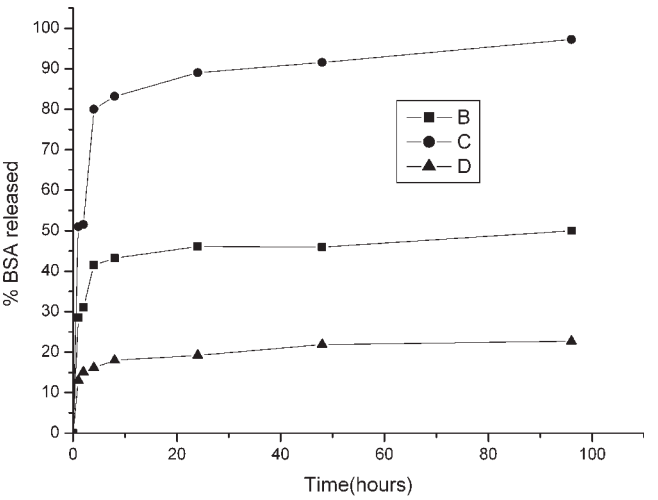

Figure 13 BSA release profiles from nanoparticles made by (B) O-HTCC, (C) physical blending of chitosan and GTMAC, and (D) chitosan.

Figure 11 shows with the TPP concentration increasing from 1 to 4 mg/mL, the zeta potentials of O-HTCC nanoparticles solution is decreasing from 50.2 to 4.6 mV. So the repel force between $—N^+(CH_3)_3$ became weaker, then the size of nanoparticles is decreasing. The conclusion from TEM and AFM was verified by zeta potentials in the step.

In vitro release of BSA from the nanoparticles

BSA loading capacity and loading efficiency profiles obtained from the chitosan and modified chitosan are illustrated by Figure 12 and Table I. O-HTCC nanoparticles have the highest loading capacity and efficiency, and the lowest ξ-potential (34.1 mV).

The preliminary protein release test from chitosan or O-HTCC nanoparticles *in vitro* proves that they had a sustained release form as shown from Figure 13. We chose pH 7.4 PBS as release medium, which simulates body fluid according to the literatures.[36,37] The *in vitro* protein release profiles obtained for each formulation showed several phases compositions.[38] A first initial burst release of 15–80% is due to the drug desorption from the particles surface. The burst release of BSA occurred instantaneously, which indicates the burst released BSA residues on the surface of chitosan nanoparticles, O-HTCC nanoparticles, and PBN. The burst release is less pronounced (15% of amount) for chitosan nanoparticles than for modified chitosan nanoparticles (42% of amount for O-HTCC and 80% of amount for PBN). The lower burst release from nanoparticles with highly crosslinked nanoparticles suggests that main BSA molecules are encapsulated inside the matrix, highly crosslinked networks enhance encapsulation. A plateau for the following one day results from the diffusion of the drug dispersed in the polymer matrix. A constant sustained release of the drug results from the diffusion of the protein through the polymer wall as well as its erosion.[35]

This difference in the release rate could be attributed to the reduced interaction between BSA and polymer, or due to the lower BSA loading of these nanoparticles. In addition, the *in vitro* release of BSA from nanoparticles containing different BSA loadings indicated that the percentage of BSA released over the time was higher for those formulations containing a lower protein loading. Consequently, these results show that there are possibilities of modulating the release rate of proteins simply by adjusting the composition of the chitosan nanoparticles or their protein loading.

TABLE I
Physicochemical Properties of Three Kinds of Nanoparticles Made with Chitosan with the Same Amounts of TPP (2 mg/mL)

	Zeta potential (mV)	BSA loading efficiency (%)	Loading capacity (%)
CS NPs	54.2 ± 1.6	20.2	14.4
O-HTCC NPs	34.1 ± 1.6	87.5	99.5
Physical blending NPs	41.7 ± 1.6	15.1	17.7

CONCLUSIONS

A number of chitosan-based colloidal systems have been revealed as very promising carriers for bioactive macromolecules. These systems boast some

attractive features, such as mucoadhesion and their capacity for the association and delivery of delicate molecules. In this study, quaternized chitosan (O-HTCC) and its nanoparticles were prepared successfully. The degree of substitution was measured by ^{1}H NMR, and it was 33.3%. TEM and AFM demonstrate and confirm that an increase in the size of chitosan nanoparticles with increasing TPP concentration. Conversely, a decrease in the size of O-HTCC nanoparticles occurs with increasing TPP concentration and under the same conditions, chitosan and O-HTCC nanoparticles are more spherical in shape. Spherical O-HTCC nanoparticles with a small diameter (about 250 nm) can be prepared by an ionic gelation method. These nanoparticles have narrow size distribution and positive surface charges. It is found that the surface charge of nanoparticles is lower when the TPP concentration is higher. High BSA loading efficiency (87.5%) and high loading capacity (99.5%) are achieved by O-HTCC nanoparticles, and the release profile of BSA from nanoparticles has an obvious burst effect and a slowly continuous release phase followed.

References

1. Jae, H. P.; Yong, W. C.; Hesson, C.; Ick, C. K.; Seo, Y. J. Biomacromolecules 2003, 4, 1087.
2. Tsai, G. J.; Su, W.-H. J Food Protect 1999, 62, 239.
3. Helander, I. M.; Nurmiaho-Lassila, E. L.; Ahvenainen, R.; Rhoades, J.; Roller, S. Int J Food Microbiol 2001, 71, 235.
4. Liu, X. F.; Guan, Y. L.; Yang, D. Z.; Li, Z.; Yao, K. D. J Appl Polym Sci 2001, 79, 1324.
5. Lim, S. H.; Hudson, S. M. J Macromol Sci Pol R 2003, C43, 223.
6. Worley, S. D.; Sun, G. Trends Polym Sci 1996, 4, 364.
7. Suzuki, K.; Saimoto, H.; Shigemasa, Y. Carbohydr Polym 1999, 39, 145.
8. Li, X.; Morimoto, M.; Sashiwa, H.; Saimoto, H.; Okamoto, Y.; Minami, S.; Shigemasa, Y. Polym Adv Technol 1999, 10, 455.
9. Li, X.; Tushima, Y.; Morimoto, M.; Saimoto, H.; Okamoto, Y.; Minami, S.; Shigemasa, Y. Polym Adv Technol 2000, 11, 176.
10. Minoru, M.; Hiroyuki, S.; Hikaru, U.; Yoshiharu, O.; Saburo, M.; Yoshihiro, S. Biomacromolecules 2001, 2, 1133.
11. Curti, E.; Britto, D. D.; Campana-Filho, S. P. Macromol Biosci 2003, 3, 571.
12. Lim, H. L.; Hudson, S. M. Carbohydr Res 2004, 339, 313.
13. Douglas, S. J.; Davis, S. S.; Illum, L. Crit Rev Ther Drug Carrier Syst 1987, 3, 233.
14. Gref, R.; Luck, M.; Quellec, P.; Marchand, M.; Dellacherie, E.; et al. Colloids Surf B 2000, 18, 301.
15. Labhasetwar, V.; Song, C.; Humphrey, W.; Shebuski, R.; Levy, R. J. J Pharm Sci 1998, 87, 1229.
16. Tan, J. S.; Butterfield, D. E.; Voycheck, C. L.; Caldwell, K. D.; Li, J. T. Biomaterials 1993, 14, 823.
17. Moghimi, S. M.; Hunter, A. C.; Murray, J. C. Pharmacol Rev 2001, 53, 283.
18. Emerich, D. F.; Thanos, C. G. Expert Opin Biol Ther 2003, 3, 655.
19. Barratt, G. Cell Mol Life Sci 2003, 60, 21.
20. Otsuka, H.; Nagasaki, Y.; Kataoka, K. Adv Drug Deliv Rev 2003, 55, 403.
21. Brigger, I.; Dubernet, C.; Couvreur, P. Adv Drug Deliv Rev 2002, 54, 631.
22. Dinesh, S.; Steven, L.; Robert, L.; Mansoor, A. Mol Pharm 2005, 2, 5, 357.
23. Jasmine, D.; Vinod, L. Int J Pharm 2002, 233, 51.
24. Kotzé, A. F.; Thanou, M. M.; Lueβen, H. L.; Boer, B. G.; Verhoef, J. C.; Junginger, H. E. Eur J Pharm Biopharm 1999, 47, 269.
25. Xu, Y. M.; Du, Y. M.; Huang, R. H.; Gao, L. P. Biomaterials 2003, 24, 5015.
26. Liu, C. G.; Desai, K. G. H.; Chen, X. G.; Park, H. J. J Agric Food Chem 2005, 53, 437.
27. Loubaki, E.; Ourevitch, M.; Sicsic, S. Eur Polym Mater 1991, 27, 311.
28. Lee, D. W.; Powers, K.; Baney, R. Carbohydr Polym 2004, 58, 371.
29. Bodmeier, R.; Chen, H. G.; Paeratakul, O. Pharm Res 1989, 6, 413.
30. Janes, K. A.; Calvo, P.; Alonso, M. J. Adv Drug Deliv Rev 2001, 4, 83.
31. Alonso, F. M. J.; Calvo, S. P.; Remunan, L. C.; Vila Jato, J. L.EP 0,860,166, A1.
32. Parka, J. H.; Kwona, S.; Namb, J. O.; Parkb, R. W.; Chunga, H.; Seoc, S. B.; Kimb, I. S.; Kwona, I. C.; Jeonga, S. Y. J Controll Release 2004, 95, 579.
33. Wolfgang, F.; Gerhard, W.; Conrad, C. Anal. Chem 2004, 76, 1909.
34. Corcoran, H.; Sung, D. J.; Banerjee, S. Ind Eng Chem Res 2001, 40, 152.
35. Bai, R. B.; Tien, C. J Colloid Interface Sci 1999, 218, 488.
36. Langer, K.; Stieneker, F.; Lambrecht, G.; Mutschles, E.; Kreuter, J. Int J Pharm 1997, 158, 211.
37. Leo, E.; Cameroni, R.; Forni, F. Int J Pharm 1999, 180, 23.
38. Lamprecht, A.; Ubrich, N.; Pérez, M. H.; Lehr, C. M.; Hoffman, M.; Maincent, P. Int J Pharm 2000, 196, 177.